



# Molecular interaction mechanisms of glycol chitosan self-healing hydrogel as a drug delivery system for gemcitabine and doxorubicin



Tzu-Hsuan Huang<sup>a</sup>, Shan-hui Hsu<sup>a,\*</sup>, Shu-Wei Chang<sup>b,c,\*</sup>

<sup>a</sup> Institute of Polymer Science and Engineering, National Taiwan University, No. 1, Sec. 4, Roosevelt Road, Taipei 10617, Taiwan

<sup>b</sup> Department of Civil Engineering, National Taiwan University, No. 1, Sec. 4, Roosevelt Road, Taipei 10617, Taiwan

<sup>c</sup> Department of Biomedical Engineering, National Taiwan University, No. 1, Sec. 4, Roosevelt Road, Taipei 10617, Taiwan

## ARTICLE INFO

### Article history:

Received 11 October 2021

Received in revised form 14 January 2022

Accepted 15 January 2022

Available online 25 January 2022

### Keywords:

Self-healing hydrogel

Anticancer drug

Molecular dynamics

Drug carrier system

## ABSTRACT

Glycol chitosan is a derivative of chitosan that has attracted attention in recent years due to its biocompatibility and biodegradability. Due to its unique biological characteristics, it has been widely used in hydrogels and biomaterials. In this study, we explored the loading efficiency of a self-healing hydrogel (GC-DP) comprising glycol chitosan (GC) and telechelic difunctional poly(ethylene glycol) (DF-PEG) for delivering the anticancer drugs gemcitabine and doxorubicin through full atomistic simulations. We also constructed full atomistic models of the two drug delivery systems at three drug concentrations of 10%, 40%, and 80% to understand how the drug concentration affects the loading efficiency and molecular structure of the GC-DP hydrogels. Through the analysis of the results, we show that the GC-DP hydrogel exhibits excellent loading efficiency for both gemcitabine and doxorubicin at all drug concentrations (10%, 40% and 80%). Our results reveal that the main mechanism of interaction between the GC-DP hydrogels and gemcitabine is van der Waals adsorption and that the dominant interactions between the GC-DP hydrogel and doxorubicin are hydrogen bonds for the D10 model and van der Waals adsorption for the D40 and D80 models. Our results provide molecular insights into how drug molecules are carried by hydrogel materials and indicate that the GC-DP hydrogel is a promising candidate for carrying both gemcitabine and doxorubicin, and thus serving as a novel drug carrier for cancer treatment.

© 2022 The Author(s). Published by Elsevier B.V. on behalf of Research Network of Computational and Structural Biotechnology. This is an open access article under the CC BY-NC-ND license (<http://creativecommons.org/licenses/by-nc-nd/4.0/>).

## 1. Introduction

Chitosan is a partially deacetylated polysaccharide derived from chitin which has been used in a variety of research fields, including biomedicine and environmental science [1,2]. Because of its non-toxicity, bioavailability and low immunogenicity, chitosan has attracted attention among polymer materials in biomedical and pharmaceutical applications [3,4]. Glycol chitosan is a derivative of chitosan that offers the advantages of biocompatibility and biodegradability, and glycol groups can enhance water solubility; therefore, it has become a potential candidate for drug delivery in many polymer carriers [5–8]. Due to its many advantages, glycol chitosan has potential for use in the development of self-healing hydrogels. A self-healing hydrogel is a material that has the ability

to repair itself when its structure is damaged. These materials have been extensively studied in the past thirty years, including their synthesis, self-healing mechanisms and in vitro encapsulation of cells [9–13]. Among them, an injectable chitosan hydrogel, which self-heals by Schiff-base linkage, has also been studied [14–18]. The self-healing chitosan hydrogel (GC-DP) was prepared by mixing glycol chitosan solution and DF-PEG solution, where glycol chitosan solution and DF-PEG solution were obtained by dissolving glycol chitosan and DF-PEG in distilled and deionized water, respectively [17,19–23]. The GC-DP hydrogel has shown feasibility in cell encapsulation and injection processes [19], a positive effect on the repair of the zebrafish embryo neural system [20], and the feasibility for use as 3D cell culture platforms [21], and it was also used as a carrier for adipose-derived mesenchymal stem cells, showing that this transplantation achieved significant cartilage regeneration and repaired the cartilage-defect area in vivo experiments [23]. Furthermore, a chitosan-fibrin-based self-healing hydrogel was fabricated, and it successfully repaired the blood circulation of the ischemic hindlimbs of mice, indicating the feasibility of applying hydrogels to vascular repair [24]. For microwave

\* Corresponding authors at: Institute of Polymer Science and Engineering, National Taiwan University, No. 1, Sec. 4, Roosevelt Road, Taipei 10617, Taiwan (S.-h. Hsu), Department of Civil Engineering, National Taiwan University, No. 1, Sec. 4, Roosevelt Road, Taipei 10617, Taiwan (S.-W. Chang).

E-mail addresses: [shhsu@ntu.edu.tw](mailto:shhsu@ntu.edu.tw) (S.-h. Hsu), [changsw@ntu.edu.tw](mailto:changsw@ntu.edu.tw) (S.-W. Chang).

tumor ablation, a chitosan-based injectable ionic hydrogel was reported to have excellent microwave susceptibility properties, providing a biocompatible and stable treatment system[22].

Owing to these excellent properties, glycol chitosan has attracted attention in controlled-release drug delivery[25]. Yang et al. used a chitosan-PEG hydrogel as a carrier for Taxol, successfully delivering the drug to the desired location. Due to its various excellent properties in the context of tumor chemotherapy, such as stability, controlled drug release and few side effects, this kind of hydrogel can be used as a drug carrier to improve the therapeutic effects of drugs[26]. The study of dual-drug-loaded magnetic hydrogels using iron oxide for magnetically induced drug release has been reported. Researchers found that the codelivery of doxorubicin and docetaxel-loaded poly(lactic-co-glycolic acid) nanoparticles by this hydrogel improved antitumor activity against triple-negative breast cancer cell lines to a greater extent than a single drug-loaded hydrogel[27].

Gemcitabine, an anticancer drug, can treat a variety of cancers, such as pancreatic cancer and bladder cancer[28,29]. Its cytotoxicity is triggered by incorporation into DNA, so controlling the dose in a safe range while simultaneously obtaining excellent loading efficiency has become an important consideration when designing a drug delivery system[30]. A study revealed that chitosan nanoparticles loaded with gemcitabine showed good antiproliferative activity[31]. Another study found that chitosan nanoparticles loaded with gemcitabine-mediating cisplatin can be used in the clinical treatment of pancreatic cancer[32]. Doxorubicin is another typical anticancer drug used in chemotherapy and is widely used in the treatment of lung cancer and breast cancer[33]. Although doxorubicin shows high antitumor activity, it attacks both normal cells and tumor cells due to its poor tumor selectivity[34,35]. In one study, nanosized self-aggregating hydrophobically modified glycol chitosan was synthesized by the chemical conjugation of doxorubicin to the backbone of glycol chitosan, and the results showed that this glycol chitosan loaded with doxorubicin effectively inhibited the growth of tumors in vivo, indicating the potential of this system as a carrier for hydrophobic drugs[6]. However, the molecular interaction mechanisms between GC-DP hydrogels and drugs, including gemcitabine and doxorubicin, remain unclear.

Molecular dynamics simulations have been widely used to help understand physical phenomena and molecular mechanisms at the atomic scale[36–39]. Drug delivery systems have also been extensively studied in the past few decades[40]. The delivery of gemcitabine and camptothecin by a system composed of lactic acid and glycolic acid has been studied; the authors explored the encapsulation efficiency of hydrophilic and hydrophobic drugs loaded with different ratios of lactic acid and glycolic acid[29]. Another study investigated the effects of the molecular weight of chitosan and temperature on a specific target drug delivery system containing carbon nanotubes and chitosan[41]. The stability and binding affinity of curcumin and chitosan nanoparticles have also been studied[37]. The ability of the thermosensitive PLGA-PEG-PLGA hydrogel to carry colchicine and irinotecan to treat myocardial infarction and promote tumor regression has also been investigated[42,43]. A series of PLGA-PEG-PLGA thermogels and camptothecin have also been prepared as drug delivery systems to enhance the solubility of this hydrophobic drug[44].

In this study, hydrophilic gemcitabine and hydrophobic doxorubicin were the anticancer drugs selected to be carried by GC-DP hydrogels. Full atomistic simulations of a GC-DP hydrogel carrying drugs from regions of low to high drug concentrations (10%, 40% and 80%) were performed to explore whether the GC-DP hydrogel is an excellent drug delivery system for both drugs and to reveal the molecular mechanisms by which the drugs are carried by

GC-DP hydrogels, with the aim of providing design strategies for GC-DP hydrogels to develop a novel drug delivery system.

## 2. Simulation methodology

In this study, full atomistic models of glycol chitosan-based self-healing hydrogels were constructed following the settings described in previous work[13]. Glycol chitosan is composed of D-glucosamine linked by  $\beta$ -(1,4) glycosidic bonds, and the degree of protonation is determined by the different number of positive charges carried by the amino group on the  $\beta$ -(1–4) glycosidic bond in the structure. The distribution of ammonium groups ( $-NH_3^+$ ) on the glycol chitosan chains is also described in the previous literature, and these groups are evenly distributed on the glycol chitosan chains. The pH value of the 20% protonated glycol chitosan was approximately 7.1, which is close to the pH value of human serum[45]. Since the absorption of most drugs occurs in the neutral environment of the gastrointestinal tract, the degree of protonation of glycol chitosan was fixed at 20%[46]. Due to protonation, both glycol chitosan and doxorubicin were positively charged, so chloride ions were added to balance the charge of the system. The schematic of the GC-DP hydrogel is shown in the top middle panel of Fig. 1. The top right panel of Fig. 1 shows the protonation sites of glycol chitosan, and the segment composition ratio of DF-PEG is presented in the middle bottom panel of Fig. 1.

The Materials Studio Amorphous Cell was used to construct the initial structure models. Table 1 shows the characteristics of our six models. Referring to the previous literature, 1.5% glycol chitosan and 1% DF-PEG were used to achieve the appropriate formula of the GC-DP hydrogels[20]. We used five chains of glycol chitosan with a degree of polymerization of 20 and protonation of 20% as the benchmark to calculate the corresponding amounts of the other components in the system. The drug concentration was calculated by Equation (1)[30].

$$\text{Drug concentration} = \frac{\text{mass of drug}}{\text{mass of polymer}} \times 100\% \quad (1)$$

Additionally, because the  $pK_a$  of doxorubicin is approximately 8.3[47], the amine group on doxorubicin would also be protonated when the pH of the environment is lower than the  $pK_a$ . Equation (2) was used to determine the proportion of protonation of doxorubicin in the system.

$$N_{\text{protonated}} = \frac{10^{pK_a - pH}}{1 + 10^{pK_a - pH}} N_{\text{total}} \quad (2)$$

where  $N_{\text{protonated}}$  is the number of protonated positions and  $N_{\text{total}}$  is the total number of ionizable functional groups.

All molecular dynamics simulations were performed by LAMMPS[48]. The consistent valence force field (CVFF) was used for all the simulations. CVFF was the forerunner of CFF and was originally applied to biological systems[49]. As Equation 3 shows, this force field included bond stretching or compression; angle bending; torsion angle twisting; out-of-plane deformation of the planar system; several cross-coupling terms between bond deformations, angle bendings, a bond deformation, an angle bending, a torsion angle twisting and the two associated angle bendings; and the nonbonded interaction between nonbonded atoms. The nonbonded interaction contained repulsive, dispersive, and Coulombic interactions. Among them,  $D_b$ ,  $H_\theta$ ,  $H_\phi$ ,  $H_\chi$  and  $F_{ij}$  are the corresponding intramolecular deformation mechanical parameters,  $\epsilon$  and  $r^*$  are the parameters of the nonbonding repulsive and dispersive interactions, and  $q_i$  is the partial charge of each atom [50].

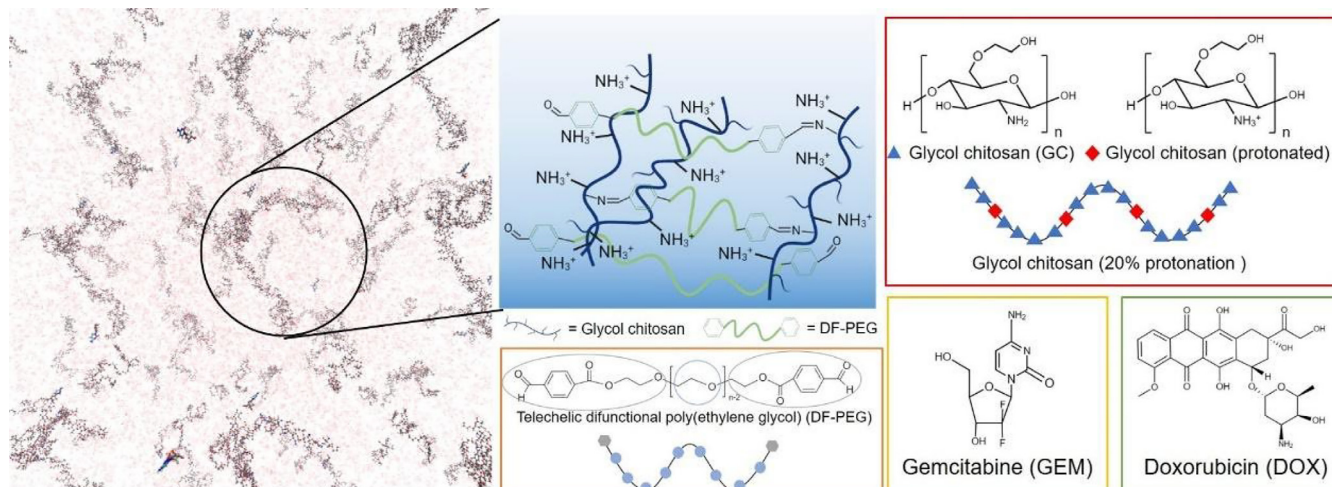


**Fig. 1.** Atomistic model of the GC-DP hydrogel. A schematic of the protonation sites on the glycol chitosan chain at 20% protonation is shown in the top right panel. A schematic of the composition ratio of DF-PEG segments and the chemical structures of gemcitabine and doxorubicin is shown in the bottom right panel.

**Table 1**

Characteristics of models; number of glycol chitosan chains, polymerization of glycol chitosan, protonation of glycol chitosan, drug concentration, number of drug molecules and number of atoms.

Models	G10	G40	G80	D10	D40	D80
Number of GC chains	5	5	5	5	5	5
Polymerization of GC	20	20	20	20	20	20
Protonation of GC (%)	20	20	20	20	20	20
Drug concentration (%)	10	40	80	10	40	80
Number of drug molecules	8	31	62	4	15	30
Atoms	110,363	110,190	111,380	110,072	109,877	111,558

$$\begin{aligned}
 E = & \sum_b D_b [1 - e^{-a(b-b_0)}] + \sum_\theta H_\theta (\theta - \theta_0)^2 + \sum_\varphi H_\varphi [1 + s \cos(n\varphi)] \\
 & + \sum_\chi H_\chi \chi^2 + \sum_b \sum_{b'} F_{bb'} (b - b_0) (b' - b'_0) + \sum_\theta \\
 & \times \sum_{\theta'} F_{\theta\theta'} (\theta - \theta_0) (\theta' - \theta'_0) + \sum_b \sum_{\theta} F_{b\theta} (b - b_0) (\theta - \theta_0) \\
 & + \sum_\varphi F_{\varphi\theta\theta'} \cos \varphi (\theta - \theta_0) (\theta' - \theta'_0) + \sum_\chi \sum_{\chi'} F_{\chi\chi'} \chi \chi' \\
 & + \sum \varepsilon \left[ \left( \frac{r^*}{r} \right)^{12} - 2 \left( \frac{r^*}{r} \right)^6 \right] + \sum \frac{q_i q_j}{\varepsilon r_{ij}} \quad (3)
 \end{aligned}$$

The simulation results of our models were analyzed by visual molecular dynamics (VMD)[51]. Equation (4) defines loading efficiency (LE), which is one way to measure the efficiency of drug carriers[30].

$$LE = \frac{\text{number of drug molecules placed within 4 angstrom from polymer chains}}{\text{total number of drug of molecules}} \quad (4)$$

The end-to-end distance is a parameter used to describe the size of the polymer. The flexibility of the polymer was judged by measuring the distance between the head and tail of the polymer chain.

The  $\pi$ -stacking interaction analysis was used to explore the influence of the benzene ring structure between the components of the model on the overall structure. In this study, as the centroid distance of the benzene ring was below 7.5 Å, it was defined as a  $\pi$ -stacking interaction[52,53]. According to the angle between the two benzene ring planes, the  $\pi$ -stacking interactions were subdivided into parallel-stacked and T-shaped structures, and the angle

classification is shown by Equation (5). D represents the possible combinations of  $\pi$ -stacking interactions.

$$D = \begin{cases} 1, (\text{centroid distance between benzene ring} \leq 7.5 \text{ \AA}) \\ \quad \text{and } (0 \leq \text{angle of plane of benzene rings} \leq 15) \\ 1, (\text{centroid distance between benzene ring} \leq 7.5 \text{ \AA}) \\ \quad \text{and } (75 \leq \text{angle of plane of benzene rings} \leq 105) \\ 0, \text{otherwise} \end{cases} \quad (5)$$

Additionally, because the structure contains many functional groups that can form hydrogen bonds, the hydrogen bonds between the carrier and drugs cannot be ignored. The average number of hydrogen bonds between the GC-DP hydrogels and drugs is computed according to the condition shown in Equation (6). Through analysis of hydrogen bonds, we can understand their influence on the interaction between the components, as well as the exact positions and combinations of functional groups that form hydrogen bonds.

$$H = \begin{cases} 1, (\text{distance}(\text{donor} \cdots \text{acceptor}) \leq 3.5 \text{ \AA}) \\ \quad \text{and } (\text{angle}(\text{H} - \text{donor} \cdots \text{acceptor}) \leq 30) \\ 0, \text{otherwise} \end{cases} \quad (6)$$

### 3. Results

#### 3.1. The loading efficiency and molecular structures of GC-DP hydrogels with gemcitabine and doxorubicin

By comparing the loading efficiencies of our gemcitabine systems and doxorubicin systems, we found that the GC-DP hydrogels

achieved good loading efficiency when carrying either gemcitabine or doxorubicin. As shown in Fig. 2A, the loading efficiency was higher than 60% at the three drug concentrations in both the gemcitabine systems and doxorubicin systems, indicating that the GC-DP hydrogel is an excellent reservoir for both drugs. The efficiency of the GC-DP hydrogels loaded with doxorubicin was higher than that of hydrogels loaded with gemcitabine. The models with 40% drug concentrations, G40 and D40, showed slightly lower loading efficiencies. Razmimanesh et al. reported simulation results of gemcitabine in chitosan, and the loading efficiencies at 10%, 40%, and 80% drug concentrations were 25%, 27%, and 10%, respectively[30]. Compared with the results of the literature, the GC-DP hydrogel showed significantly higher loading efficiency than chitosan at the three drug concentrations.

To understand how the drug molecules were loaded by the GC-DP hydrogels, we analyzed the number of drugs loaded by glycol chitosan and DF-PEG. The proportion of loading efficiency provided by glycol chitosan or DF-PEG for gemcitabine systems is shown in Fig. 2B. In G10, more gemcitabine molecules were loaded by glycol chitosan, but the proportions of gemcitabine loaded by glycol chitosan or DF-PEG remained almost the same as the drug concentration increased. In the D10 model, there were also more doxorubicin molecules loaded by glycol chitosan, but in the D40 and D80 models, the loading efficiency provided by DF-PEG was significantly higher (Fig. 2C). These results indicate that both glycol chitosan and DF-PEG play important roles in loading doxorubicin and gemcitabine.

From the analysis of the end-to-end distance detailed in Fig. 2D, we found that the glycol chitosan chains were more extended in the doxorubicin systems than in the gemcitabine systems. The change in drug concentration had a slight effect on the end-to-end distance of the glycol chitosan chains in either the gemcitabine system or the doxorubicin system. The model with a drug concentration of 40% had the smallest average end-to-end distances, which were 47.5 Å for G40 and 63.6 Å for D40. These results indicate that the loading of doxorubicin or gemcitabine does not affect the molecular structure of the GC-DP hydrogels.

### 3.2. Molecular interaction mechanisms between the GC-DP hydrogels and gemcitabine

The adsorption behaviors of gemcitabine were evaluated by analyzing the hydrogen bonds,  $\pi$ -stacking interactions and van der Waals adsorption between the GC-DP hydrogels and gemcitabine. Fig. 3A shows the proportion of loading efficiency for the three interactions of G10. Gemcitabine (58.4%) was loaded through van der Waals adsorption, which was the main interaction between the GC-DP hydrogels and gemcitabine. The secondary interaction was the  $\pi$ -stacking interaction at 13.6%, while only 6% of loading occurred through hydrogen bonds. This result indicates that the major interactions between the GC-DP hydrogels and gemcitabine are van der Waals interactions.

For hydrogen bond analysis, we divided the structure of glycol chitosan into the main group and the side group, where the main

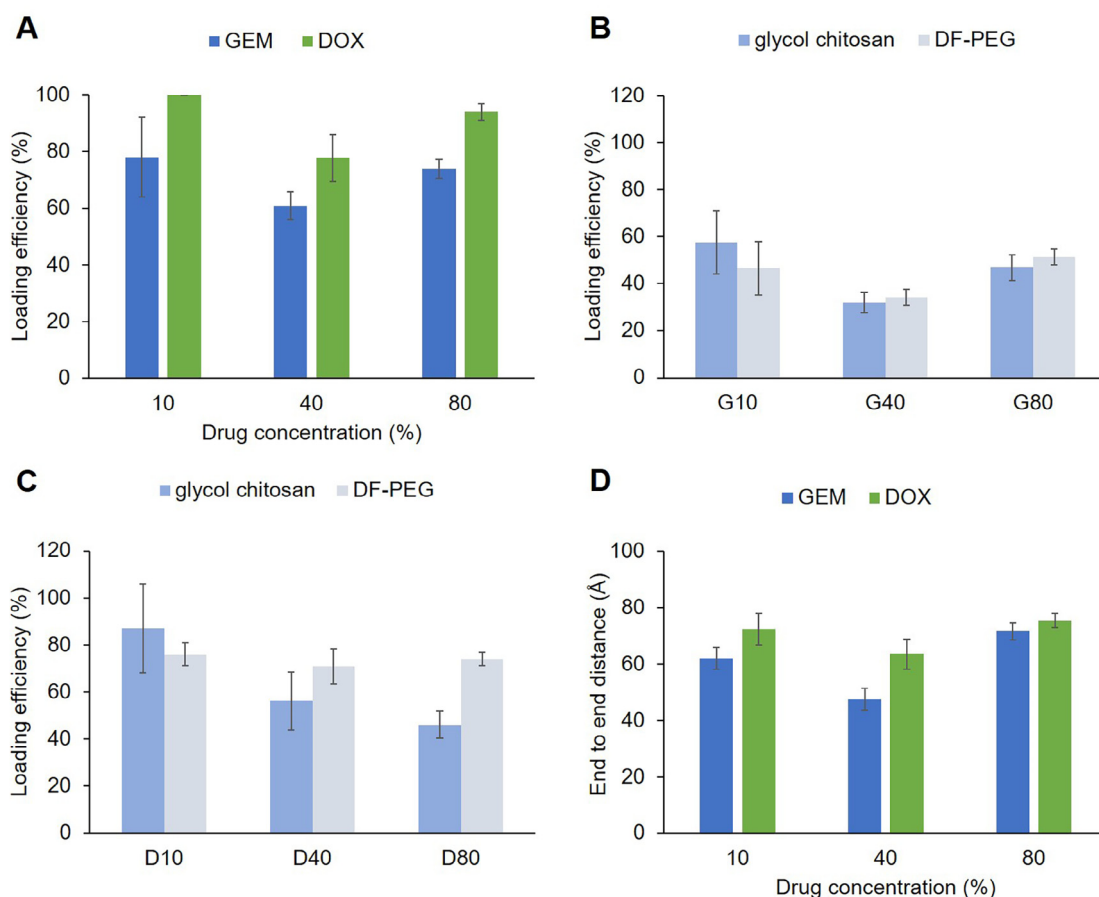


**Fig. 2.** A The loading efficiency of the GC-DP hydrogels for gemcitabine and doxorubicin. B The proportion of the loading efficiency provided by glycol chitosan or DF-PEG for gemcitabine systems. C The proportion of the loading efficiency provided by glycol chitosan or DF-PEG for doxorubicin systems. D Analysis of the end-to-end distance of glycol chitosan chains in each system.

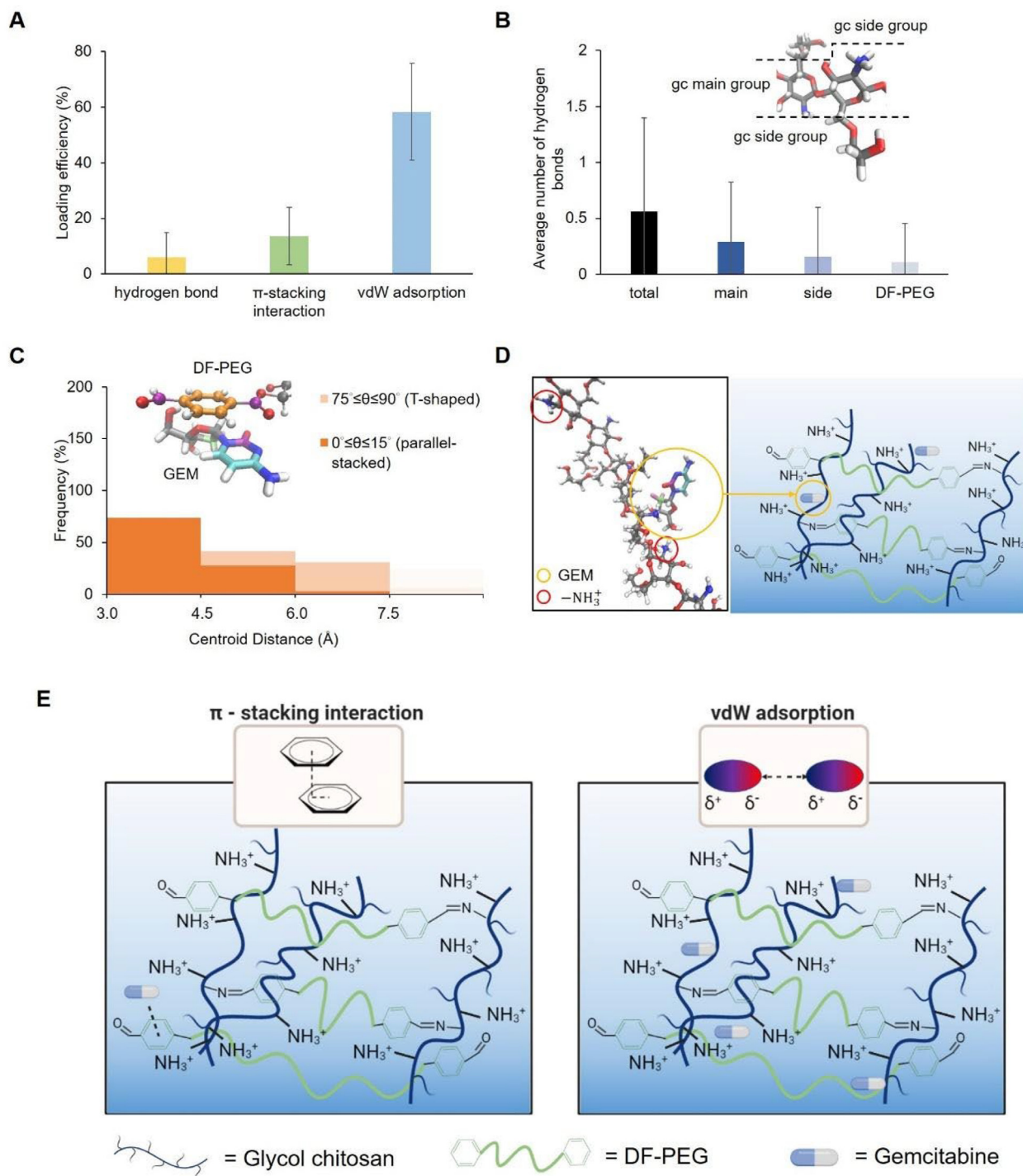


**Fig. 3.** **A** Distribution of gemcitabine molecules loaded through hydrogen bonds,  $\pi$ - $\pi$  interactions and van der Waals adsorption for the G10 model. **B** Analysis of the average number of hydrogen bonds between the GC-DP hydrogels and gemcitabine for the G10 model. **C** Distribution of the centroid distance between the loaded gemcitabine molecules and benzene rings of the DF-PEG molecules for the G10 model. The transparent sections indicate a lack of  $\pi$ -stacking interactions between the rings. The frequency represents the average number of  $\pi$ -stacking interactions that appear in each frame. **D** Snapshots of van der Waals adsorption in the G10 model. **E** Schematic of the interaction mechanisms between the GC-DP hydrogels and gemcitabine. Adapted from “Blank Panels (1 × 3)” by BioRender.com (2021). Retrieved from <https://app.biorender.com/biorender-templates>.

group contained  $\beta$ -(1–4)-linked D-glucosamine and the side group included glycol chains, as shown in Fig. 3B. Hydrogen bonds are mainly formed at the main group of glycol chitosan, but the average number of hydrogen bonds between the GC-DP hydrogels and gemcitabine is small.

We further analyzed the  $\pi$ -stacking interactions between the cytosine ring of gemcitabine and the benzene rings of DF-PEG. The distributions of the centroid distance and the angle between

the plane of the cytosine ring and the plane of the benzene ring were analyzed and are shown in Fig. 3C. The  $\pi$ -stacking interactions were found between DF-PEG and gemcitabine molecules at 147% frequency, and the conformation was dominated by parallel-stacked  $\pi$ -stacking interactions.

We classified the loading interactions aside from the hydrogen bonds and  $\pi$ -stacking interactions as van der Waals adsorption. In the simulation trajectories, the main location of van der Waals

adsorption was near the protonated amine group of the glycol chitosan chains (Fig. 3D).

In summary, our results show that gemcitabine is mainly loaded by GC-DP hydrogels through two mechanisms of interactions,  $\pi$ -stacking interactions and van der Waals adsorption, as illustrated in Fig. 3E.

We also performed the same analysis for the G40 and G80 models, and the detailed results are shown in Fig. 4. Fig. 4A shows that the most vital interaction between the GC-DP hydrogels and gemcitabine was van der Waals adsorption, followed by  $\pi$ -stacking interactions and hydrogen bonds.

As shown in Fig. 4B, the main hydrogen bond between the GC-DP hydrogel and gemcitabine is also located in the main group of glycol chitosan in G40 and G80. Even when the drug concentration was significantly increased, the average number of hydrogen bonds between the GC-DP hydrogels and gemcitabine remained small, indicating that hydrogen bonds were not the primary interactions at all drug concentrations.

The frequency of  $\pi$ -stacking interactions gradually increased with increasing drug concentration, and the interaction frequencies in G40 and G80 were 327% and 1000%, respectively. The  $\pi$ -

stacking interaction was still dominated by parallel-stacked conformations in G40 and G80 (Fig. 4C).

### 3.3. Molecular interaction mechanisms between the GC-DP hydrogels and doxorubicin

The interactions between the GC-DP hydrogels and doxorubicin were also studied. We calculated the distribution of the drug loading interactions of D10, as shown in Fig. 5A, and all three interactions between the GC-DP hydrogels and doxorubicin were observed. It was found that 48% were hydrogen bonds, 22% were  $\pi$ -stacking interactions, and 30% were van der Waals adsorption interactions. This result reveals that hydrogen bonds represented the major interaction, while  $\pi$ -stacking interactions and van der Waals adsorption were secondary interactions. It is worth noting that although the GC-DP hydrogel is an excellent drug carrier for both gemcitabine and doxorubicin, the molecular interactions are different.

The average number of hydrogen bonds between the GC-DP hydrogels and doxorubicin was 2.85, as shown in Fig. 5B. We found that the average number of hydrogen bonds between glycol chi-

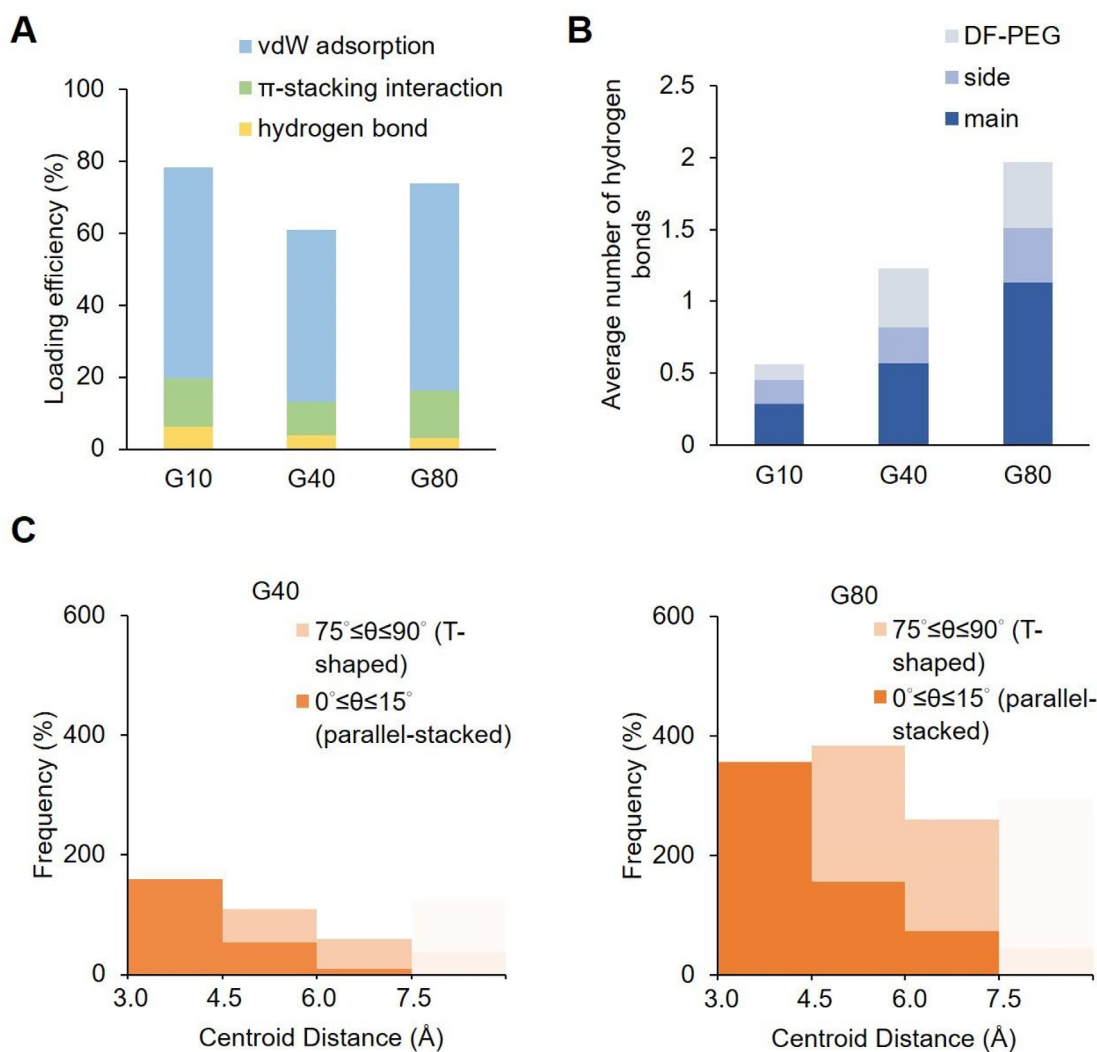


**Fig. 4.** A Distribution of gemcitabine molecules loaded through hydrogen bonds,  $\pi$ -stacking interactions and van der Waals adsorption. B Distribution of the average number of hydrogen bonds between the GC-DP hydrogels and gemcitabine. C Distribution of the centroid distance between the cytosine rings in the loaded gemcitabine molecules and the benzene rings in the DF-PEG molecules in the G40 and G80 models.

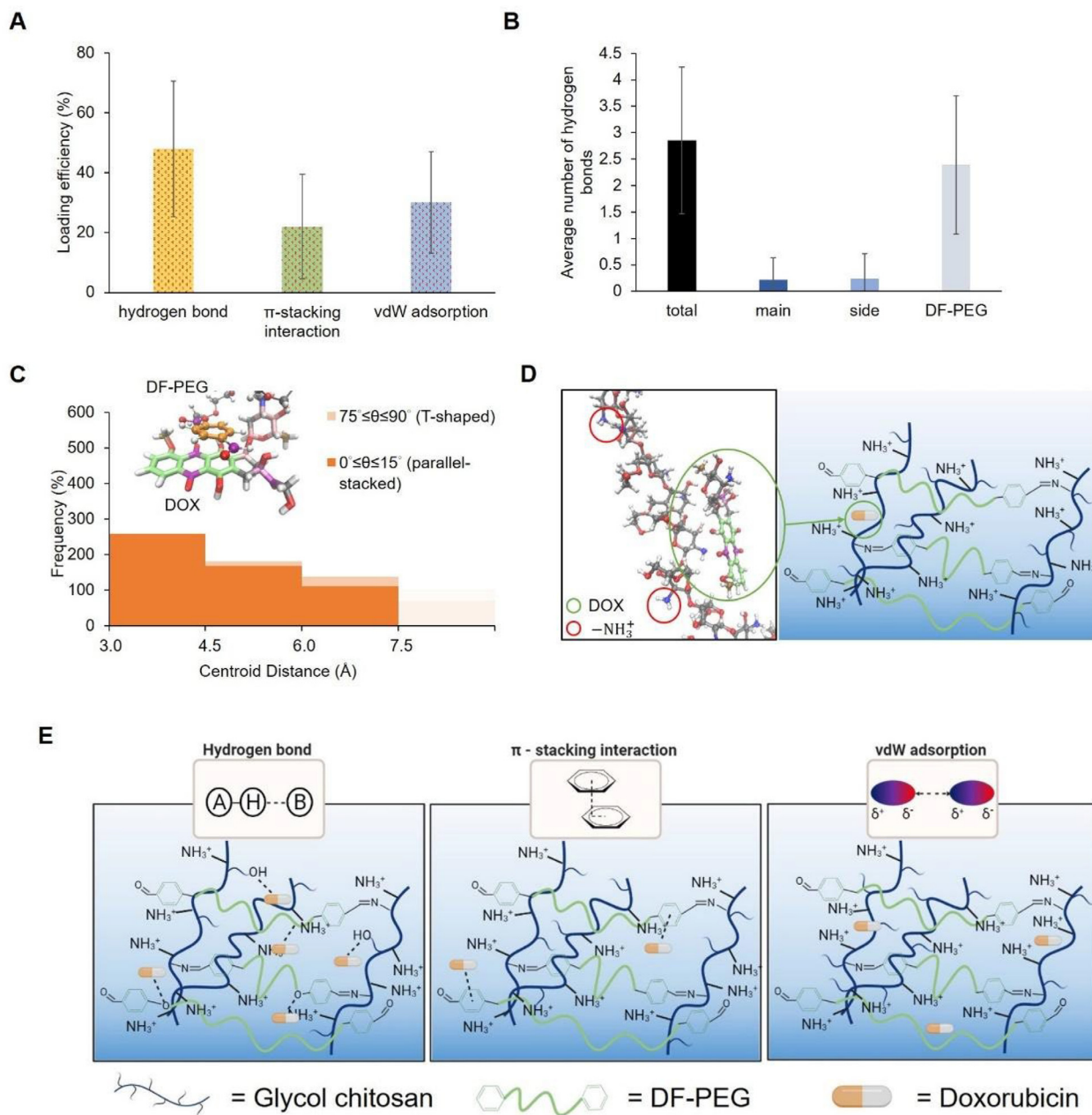


**Fig. 5.** **A** Distribution of doxorubicin molecules loaded through hydrogen bonds,  $\pi$ -stacking interactions and van der Waals adsorption for the D10 model. **B** Analysis of the average number of hydrogen bonds between the GC-DP hydrogels and doxorubicin for the D10 model. **C** Distribution of the centroid distance between the benzene rings in loaded doxorubicin molecules and the benzene rings in DF-PEG molecules for the D10 model. **D** Snapshots of van der Waals adsorption in the D10 model. **E** Schematic of the interaction mechanisms between the GC-DP hydrogels and doxorubicin. Adapted from “Blank Panels (1 × 3)” by BioRender.com (2021). Retrieved from <https://app.biorender.com/biorender-templates>.

tosan and doxorubicin was only 0.46, while that between DF-PEG and doxorubicin was 2.39, indicating that the hydrogen bonds were mainly formed between DF-PEG and doxorubicin.

Next, the distribution of  $\pi$ -stacking interactions between DF-PEG and doxorubicin in the D10 model was calculated, as shown in Fig. 5C. As discussed earlier regarding the  $\pi$ -stacking interaction of the gemcitabine systems, we defined the angle between the plane of the benzene ring of doxorubicin and DF-PEG as  $\theta$ . The results obtained in Fig. 5C show that the total frequency was 575%, and that the conformation was dominated by parallel-stacked  $\pi$ -stacking interactions.

We observed from the simulation trajectories that the location of van der Waals adsorption between the GC-DP hydrogels and

doxorubicin molecules was also near the protonated amine groups of the glycol chitosan chain (Fig. 5D).

Fig. 5E demonstrates the three interaction mechanisms of the D10 model. Among the interactions, the hydrogen bond was mainly formed by the ether group of DF-PEG and the hydroxyl group of doxorubicin, and the  $\pi$ -stacking interaction was dominated by parallel  $\pi$ -stacking between the benzene rings of DF-PEG and doxorubicin. The location of van der Waals adsorption near the protonated amine groups of the glycol chitosan chain was observed from the simulation trajectories.

We calculated the distribution of the drug loading interactions in the D40 and D80 models, as shown in Fig. 6A. In the D40 model, only 19.5% of these interactions were hydrogen bonds, which is

lower than the loading efficiency of  $\pi$ -stacking interactions and van der Waals adsorption. In the D80 model, 53.3% of the interactions were van der Waals adsorption, indicating that the most important interaction changed from hydrogen bonding to van der Waals adsorption when the drug concentration was higher.

The increase in drug concentration exerts a significant effect on the increase in the average number of hydrogen bonds shown in Fig. 6B. The average numbers of hydrogen bonds between the GC-DP hydrogels and doxorubicin on D40 and D80 were 3.52 and 9.59, respectively. Hydrogen bonds were also mainly formed between DF-PEG and doxorubicin. Analysis of the hydrogen bonding formation positions revealed that when a certain doxorubicin molecule interacted with the GC-DP hydrogel through hydrogen bonds, more than two hydrogen bonds may have formed between them simultaneously, which meant that the increase in drug concentration enhanced the local hydrogen bond interaction between the GC-DP hydrogels and doxorubicin.

In Fig. 6C, the frequencies of  $\pi$ -stacking interactions in D40 and D80 are 1052% and 2075%, respectively, indicating that the frequency of  $\pi$ -stacking interactions increases with increasing drug concentration. The  $\pi$ -stacking interactions in D40 and D80 were also dominated by parallel-stacked conformations.

### 3.4. Diffusivity of gemcitabine and doxorubicin in the GC-DP hydrogels

The diffusivity of drug molecules in all systems was calculated by plotting the MSD curves. Fig. 7A shows the MSD diagrams for the diffusion of gemcitabine and doxorubicin molecules in the GC-DP hydrogels at different drug concentrations. The curves with increasing MSD indicate that the drug molecules continuously diffused through the system throughout the simulation time. We calculated the values of the diffusion coefficients in each system, as shown in Fig. 7B. For gemcitabine systems, it was found that the highest diffusion coefficient was measured for G10 ( $2.34 \times 10^{-5} \text{ cm}^2/\text{s}$ ), and the smallest diffusion coefficient was observed for G40 ( $1.76 \times 10^{-5} \text{ cm}^2/\text{s}$ ). However, in the doxorubicin systems, the highest diffusion coefficient was found for D40 ( $1.24 \times 10^{-5} \text{ cm}^2/\text{s}$ ), followed by D80 ( $0.96 \times 10^{-5} \text{ cm}^2/\text{s}$ ), and the slowest diffusion was measured for D10 ( $0.82 \times 10^{-5} \text{ cm}^2/\text{s}$ ). The results also confirmed the results obtained from the analysis of the loading efficiency. Therefore, from the MSD analysis, we know that the diffusion of gemcitabine was relatively rapid, while the diffusion of doxorubicin was relatively slow, possibly due to the stronger interactions between the GC-DP hydrogels and doxorubicin. Falk et al. reported that the diffusion coefficient of paraceta-

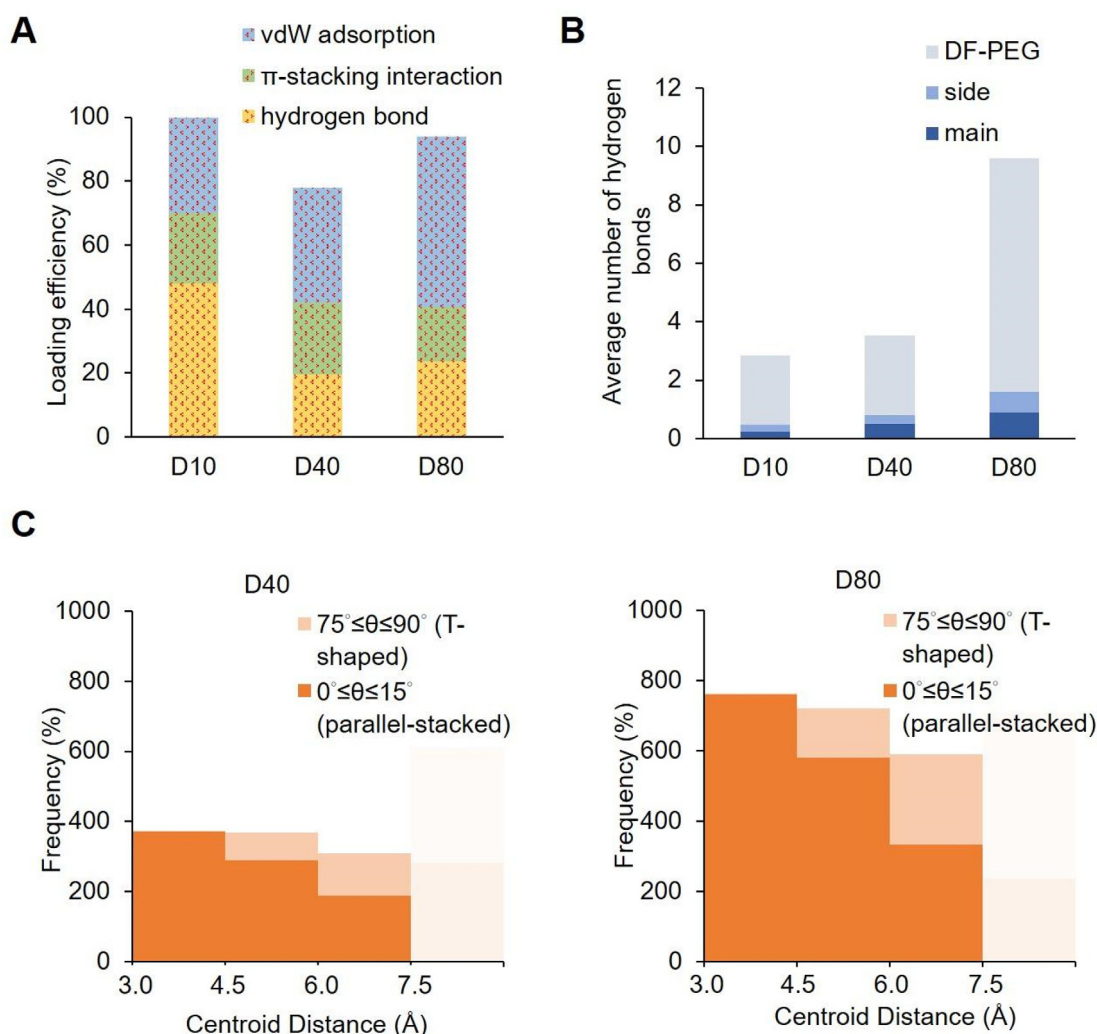


**Fig. 6.** **A** Distribution of gemcitabine molecules loaded through hydrogen bonds,  $\pi$ -stacking interactions and van der Waals adsorption for D40 and D80. **B** Analysis of the average number of hydrogen bonds between the GC-DP hydrogels and doxorubicin for D40 and D80. **C** Distribution of the centroid distance between the benzene rings in the loaded doxorubicin molecules and the benzene rings in the DF-PEG molecules for D40 and D80.

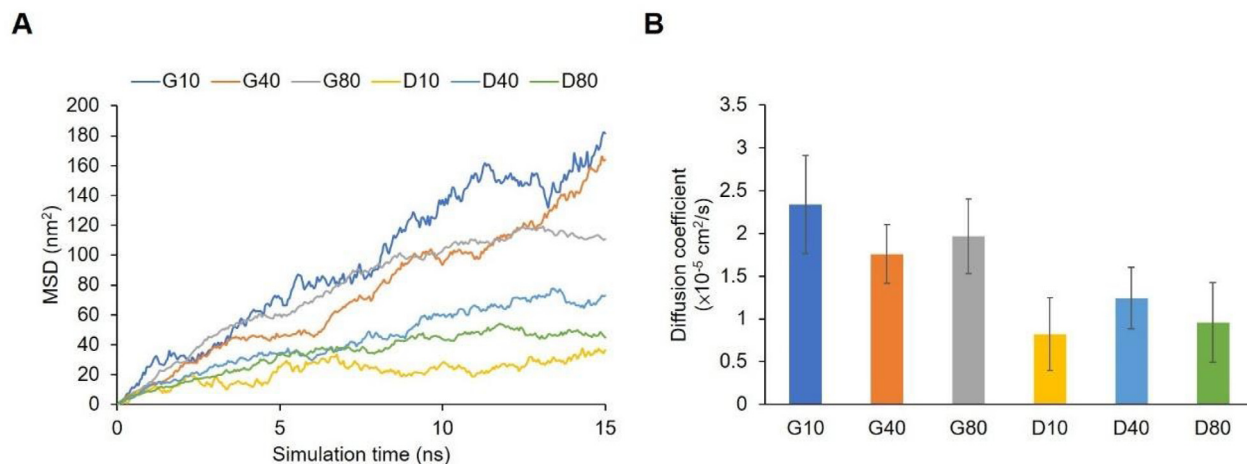


**Fig. 7.** **A** MSD diagrams for the diffusion of gemcitabine and doxorubicin molecules in the GC-DP hydrogels. **B** Diffusion coefficients of gemcitabine and doxorubicin in each system with different drug concentrations.

mol in chitosan hydrogels was  $3 \times 10^{-5} \text{cm}^2/\text{s}$  [54], and Mahdavi et al. reported that the diffusion coefficients of doxorubicin in GO-13 and GO-16 were  $1.3 \times 10^{-5} \text{cm}^2/\text{s}$  and  $1.7 \times 10^{-5} \text{cm}^2/\text{s}$  [33], respectively. The diffusion coefficients of gemcitabine and doxorubicin in the GC-DP hydrogel were close to the results reported in the literature.

#### 4. Conclusion

In this study, we explored the loading efficiency of GC-DP hydrogels for gemcitabine and doxorubicin through bottom-up full atomistic simulations. The GC-DP hydrogels showed excellent loading efficiency, indicating that they had the potential to carry both drugs. We also explored the molecular interaction mechanisms between the GC-DP hydrogels and both drugs to reveal molecular insights into how drug molecules are loaded by the hydrogel. Our results showed that although the GC-DP hydrogels had high loading efficiency for both drugs, the molecular interactions between the drugs and the hydrogel were different. The molecular interaction between the GC-DP hydrogel and gemcitabine was dominated by van der Waals adsorption, and the primary location of adsorption was near the protonated amine groups of the glycol chitosan chains. In contrast, the dominant interaction between the GC-DP hydrogels and doxorubicin was affected by the drug concentration; hydrogen bonding was the main interaction in the D10 model, and van der Waals adsorption represented the main interaction for the D40 and D80 models. The hydrogen bond formed between the ether group of DF-PEG and doxorubicin was the most common interaction, and van der Waals adsorption also usually appeared near the protonated amine groups of the glycol chitosan chains. In addition, the parallel  $\pi$ -stacking interaction was an important molecular interaction between the GC-DP hydrogels and doxorubicin. Since hydrogen bonds and  $\pi$ -stacking interactions mainly occurred between DF-PEG and doxorubicin, DF-PEG might play an important role when GC-DP hydrogels carry doxorubicin. Our results reveal the important molecular insight that a good crosslinking agent, for example, DF-PEG in GC-DP hydrogels, can not only provide better mechanical properties for self-healing hydrogels but also play an important role in the loading of drug molecules.

We also calculated the diffusivity of drugs in all of the systems. The diffusion of doxorubicin molecules was slower than that of gemcitabine molecules, which might be attributed to the hydrogen bonds and  $\pi$ -stacking interactions between the GC-DP hydrogels

and doxorubicin. Understanding the loading efficiency of the GC-DP hydrogels and the molecular interaction mechanism between hydrogels and drugs provides crucial fundamental knowledge for designing novel drug delivery systems, thus promoting the application of self-healing hydrogels in biomaterials and biomedicine.

#### CRedit authorship contribution statement

**Tzu-Hsuan Huang:** Software, Formal analysis, Investigation, Writing – original draft. **Shan-hui Hsu:** Conceptualization, Supervision, Writing – review & editing. **Shu-Wei Chang:** Conceptualization, Methodology, Writing – review & editing, Supervision.

#### Declaration of Competing Interest

The authors declare that they have no known competing financial interests or personal relationships that could have appeared to influence the work reported in this paper.

#### Acknowledgments

This work was supported by the Ministry of Science and Technology, Taiwan [109-2224-E-007-003, 110-2636-E-002-013], and the National Taiwan University [109L891002].

#### References

- [1] Nam HY, Kwon SM, Chung H, Lee SY, Kwon SH, et al. Cellular uptake mechanism and intracellular fate of hydrophobically modified glycol chitosan nanoparticles. *J Control Rel* 2009;135:259–67.
- [2] Yang HC, Hon MH. The effect of the molecular weight of chitosan nanoparticles and its application on drug delivery. *Microchem J* 2009;92:87–91.
- [3] Safdar R, Omar AA, Arunagiri A, Regupathi I, Thanabalan M. Potential of Chitosan and its derivatives for controlled drug release applications – A review. *J Drug Deliv Sci Technol* 2019;49:642–59.
- [4] Philippova OE, Korchagina EV. Chitosan and its hydrophobic derivatives: Preparation and aggregation in dilute aqueous solutions. *Polym Sci Ser A* 2012;54:552–72.
- [5] Kim JH, Kim YS, Park K, Lee S, Nam HY, et al. Antitumor efficacy of cisplatin-loaded glycol chitosan nanoparticles in tumor-bearing mice. *J Control Rel* 2008;127:41–9.
- [6] Park JH, Kwon S, Lee M, Chung H, Kim JH, et al. Self-assembled nanoparticles based on glycol chitosan bearing hydrophobic moieties as carriers for doxorubicin: In vivo biodistribution and anti-tumor activity. *Biomaterials* 2006;27:119–26.
- [7] Kim K, Kwon S, Park JH, Chung H, Jeong SY, et al. Physicochemical Characterizations of Self-Assembled Nanoparticles of Glycol Chitosan–Deoxycholic Acid Conjugates. *Biomacromolecules* 2005;6:1154–8.

- [8] Trapani A, Sitterberg J, Bakowsky U, Kissel T. The potential of glycol chitosan nanoparticles as carrier for low water soluble drugs. *Int J Pharm* 2009;375:97–106.
- [9] South AB, Lyon LA. Autonomic Self-Healing of Hydrogel Thin Films. *Angew Chem Int Ed* 2010;49:767–71.
- [10] Frey S, Görllich D. FG/FxFG as well as GLFG repeats form a selective permeability barrier with self-healing properties. *EMBO J* 2009;28:2554–67.
- [11] Roberts MC, Hanson MC, Massey AP, Karren EA, Kiser PF. Dynamically Restructuring Hydrogel Networks Formed with Reversible Covalent Crosslinks. *Adv Mater* 2007;19:2503–7.
- [12] Lu HD, Charati MB, Kim IL, Burdick JA. Injectable shear-thinning hydrogels engineered with a self-assembling Dock-and-Lock mechanism. *Biomaterials* 2012;33:2145–53.
- [13] Hsu SC, Hsu SH, Chang SW. Effect of pH on Molecular Structures and Network of Glycol Chitosan. *ACS Biomater Sci Eng* 2020;6:298–307.
- [14] Liu Y, Hsu SH. Synthesis and biomedical applications of self-healing hydrogels. *Front Chem* 2018;6:449.
- [15] Xu J, Liu Yi, Hsu S-H. Hydrogels Based on Schiff Base Linkages for Biomedical Applications. *Molecules* 2019;24(16):3005. <https://doi.org/10.3390/molecules24163005>.
- [16] Xu Y, Li Y, Chen Q, Fu L, Tao L, et al. Injectable and Self-Healing Chitosan Hydrogel Based on Iminic Bonds: Design and Therapeutic Applications. *Int J Mol Sci* 2018;19:2198.
- [17] Zhang Y, Tao L, Li S, Wei Y. Synthesis of Multiresponsive and Dynamic Chitosan-Based Hydrogels for Controlled Release of Bioactive Molecules. *Biomacromolecules* 2011;12:2894–901.
- [18] Cheng KC, Huang CF, Wei Y, Hsu SH. Novel chitosan–cellulose nanofiber self-healing hydrogels to correlate self-healing properties of hydrogels with neural regeneration effects. *NPG Asia Mater* 2019;11:25.
- [19] Yang B, Zhang Y, Zhang X, Tao L, Li S, et al. Facilely prepared inexpensive and biocompatible self-healing hydrogel: a new injectable cell therapy carrier. *Polym Chem* 2012;3:3235–8.
- [20] Tseng TC, Tao L, Hsieh FY, Wei Y, Chiu IM, et al. An Injectable, Self-Healing Hydrogel to Repair the Central Nervous System. *Adv Mater* 2015;27:3518–24.
- [21] Li Y, Zhang Y, Wei Y, Tao L. Preparation of Chitosan-based Injectable Hydrogels and Its Application in 3D Cell Culture. *J Vis Exp* 2017;127:e56253.
- [22] Wang J, Wang D, Yan H, Tao L, Wei Y, et al. An injectable ionic hydrogel inducing high temperature hyperthermia for microwave tumor ablation. *J Mater Chem B* 2017;5:4110–20.
- [23] Yang J, Jing X, Wang Z, Liu X, Zhu X, et al. In vitro and in vivo Study on an Injectable Glycol Chitosan/Dibenzaldehyde-Terminated Polyethylene Glycol Hydrogel in Repairing Articular Cartilage Defects. *Front Bioeng Biotechnol* 2021;9:607709.
- [24] Hsieh FY, Tao L, Wei Y, Hsu SH. A novel biodegradable self-healing hydrogel to induce blood capillary formation. *NPG Asia Mater* 2017;9:e363.
- [25] Riva R, Ragelle H, des Rieux A, Duhem N, Jerome C, et al. Chitosan and Chitosan Derivatives in Drug Delivery and Tissue Engineering. *Adv Polym Sci* 2011;244:19–44.
- [26] Yang L, Li Y, Gou Y, Wang X, Zhao X, et al. Improving tumor chemotherapy effect using an injectable self-healing hydrogel as drug carrier. *Polym Chem* 2017;8:5071–6.
- [27] Xie W, Gao Q, Guo Z, Wang D, Gao F, et al. Injectable and Self-Healing Thermosensitive Magnetic Hydrogel for Asynchronous Control Release of Doxorubicin and Docetaxel to Treat Triple-Negative Breast Cancer. *ACS Appl Mater Interfaces* 2017;9:33660–73.
- [28] Paroha S, Verma J, Dubey RD, Dewangan RP, Molugulu N, et al. Recent advances and prospects in gemcitabine drug delivery systems. *Int J Pharm* 2021;592:120043.
- [29] Ansari M, Moradi S, Shahlaei M. A molecular dynamics simulation study on the mechanism of loading of gemcitabine and camptothecin in poly lactic-co-glycolic acid as a nano drug delivery system. *J Mol Liq* 2018;269:110–8.
- [30] Razmimanesh F, Amjad-Iranagh S, Modarress H. Molecular dynamics simulation study of chitosan and gemcitabine as a drug delivery system. *J Mol Model* 2015;21:165.
- [31] Parsian M, Unsoy G, Mutlu P, Yalcin S, Tezcaner A, et al. Loading of Gemcitabine on chitosan magnetic nanoparticles increases the anti-cancer efficacy of the drug. *Eur J Pharmacol* 2016;784:121–8.
- [32] Yu H, Song H, Xiao J, Chen H, Jin X, et al. The effects of novel chitosan-targeted gemcitabine nanomedicine mediating cisplatin on epithelial mesenchymal transition, invasion and metastasis of pancreatic cancer cells. *Biomed Pharmacother* 2017;96:650–8.
- [33] Mahdavi M, Rahmani F, Nouranian S. Molecular simulation of pH-dependent diffusion, loading, and release of doxorubicin in graphene and graphene oxide drug delivery systems. *J Mater Chem B* 2016;4:7441–51.
- [34] Hrubý MC, Koňák Č, Ulbrich K. Polymeric micellar pH-sensitive drug delivery system for doxorubicin. *J Control Rel* 2005;103:137–48.
- [35] Li J, Ying S, Ren H, Dai J, Zhang L, et al. Molecular dynamics study on the encapsulation and release of anti-cancer drug doxorubicin by chitosan. *Int J Pharm* 2020;580:119241.
- [36] van Gunsteren WF, Berendsen HJC. Computer Simulation of Molecular Dynamics: Methodology, Applications, and Perspectives in Chemistry. *Angew Chem Int Ed* 1990;29:992–1023.
- [37] Yadav P, Bandyopadhyay A, Chakraborty A, Sarkar K. Enhancement of anticancer activity and drug delivery of chitosan-curcumin nanoparticle via molecular docking and simulation analysis. *Carbohydr Polym* 2018;182:188–98.
- [38] Wen CH, Hsu SC, Hsu SH, Chang SW. Molecular Structures and Mechanisms of Waterborne Biodegradable Polyurethane Nanoparticles. *Comput Struct Biotechnol J* 2019;17:110–7.
- [39] Esalmi M, Nikkha S, Hashemianzadeh SM, Sajadi SAS. The compatibility of Tacriner molecule with poly(n-butylcyanoacrylate) and Chitosan as efficient carriers for drug delivery A molecular dynamics study. *Eur J Pharm Sci* 2016;82:79–85.
- [40] Subashini M, Devarajan PV, Sonavane GS, Doble M. Molecular dynamics simulation of drug uptake by polymer. *J Mol Model* 2011;17:1141–7.
- [41] Rungnim C, Rungrotmongkol T, Hannongbua S, Okumura H. Replica exchange molecular dynamics simulation of chitosan for drug delivery system based on carbon nanotube. *J Mol Graphics Model* 2013;39:183–92.
- [42] Chen Y, Shi J, Zhang Y, Miao J, Zhao Z, et al. An injectable thermosensitive hydrogel loaded with an ancient natural drug colchicine for myocardial repair after infarction. *J Mater Chem B* 2020;8:980–92.
- [43] Ci T, Chen L, Yu L, Ding J. Tumor regression achieved by encapsulating a moderately soluble drug into a polymeric thermogel. *Sci Rep* 2014;4:5473.
- [44] Yu LCGT, Zhang H, Ding JD. Injectable block copolymer hydrogels for sustained release of a PEGylated drug. *Int J Pharm* 2007;348:95–106.
- [45] Schwalfenberg GK. The alkaline diet: is there evidence that an alkaline pH diet benefits health? *J Environ Public Health* 2012;2012:1–7.
- [46] Ways TMM, Lau WM, Khutoryanskiy VV. Chitosan and Its Derivatives for Application in Mucoadhesive Drug Delivery Systems. *Polymers* 2018;10:267.
- [47] Adnan A, Lam R, Chen H, Lee J, Schaffer DJ, et al. Atomistic Simulation and Measurement of pH Dependent Cancer Therapeutic Interactions with Nanodiamond Carrier. *Mol Pharm* 2011;8:368–74.
- [48] Plimpton S. Fast Parallel Algorithms for Short-Range Molecular Dynamics. *J Comput Phys* 1995;117:1–19.
- [49] Mark JE, editor. *Physical Properties of Polymers Handbook*. New York, NY: Springer New York; 2007.
- [50] Dauber-Osguthorpe P, Roberts VA, Osguthorpe DJ, Wolff J, Genest M, et al. Structure and energetics of ligand binding to proteins: Escherichia coli dihydrofolate reductase-trimethoprim, a drug-receptor system. *Proteins Struct Funct Bioinf* 1988;4:31–47.
- [51] Humphrey W, Dalke A, Schulten K. Visual molecular dynamics. *J Mol Graph* 1996;14(1):33–8.
- [52] McGaughey GB, Gagné M, Rappé AK. Pi-stacking interactions: alive and well in proteins. *J Biol Chem* 1998;273:15458–63.
- [53] Yuki H, Tanaka Y, Hata M, Ishikawa H, Neya S, et al. Implementation of  $\pi$ - $\pi$  Interactions in Molecular Dynamics Simulation. *J Comput Chem* 2007;28:1091–9.
- [54] Falk B, Garramone S, Shivkumar S. Diffusion coefficient of paracetamol in a chitosan hydrogel. *Mater Lett* 2004;58:3261–5.